Ind. J. Pharm. Edu. Res., 2023; 57(2s):s442-s452.
https://www.ijper.org

Original Article

Molecular Docking and *in vitro* Enzyme Assay of Bioactive Compound Isolated from *Rhus tripartite* Collected from Hail Region of Saudi Arabia as Potential Anti-Diabetic Agent

Aziz Unnisa[1], Rama Devi Kunduru[2], Suresh Babu Jandrajupalli[3], Badria Awad Elamine[4], Humerah Banu[5], Anupama Baratam[6,*], Sharukh Khan[7]

[1]Department of Pharmaceutical Chemistry, College of Pharmacy, University of Hail, Hail, SAUDI ARABIA.
[2]Department of Biology, College of Sciences, University of Hail, Hail, SAUDI ARABIA.
[3]Department of Preventive Dental Sciences, College of Dentistry, University of Hail, SAUDI ARABIA.
[4]Department of Radiology, College of Applied Medical Sciences, University of Hail, Hail, SAUDI ARABIA.
[5]Department of Clinical Nutrition, College of Applied Medicine, University of Hail, Hail, SAUDI ARABIA.
[6]Department of Pharmaceutical Chemistry, K.V.S.R. Siddhartha College of Pharmaceutical Sciences, Andhra Pradesh, INDIA.
[7]Department of Pharmaceutical Chemistry, N.B.S. Institute of Pharmacy, Ausa, Maharashtra, INDIA.

ABSTRACT

Aim: In the present investigation, we have studied the inhibitory potential of a bioactive compound isolated from *Rhus tripartite* on Glucokinase (GK), Dipeptidyl Peptidase-IV (DPP-IV), alpha-glucosidase, and alpha-amylase enzymes. **Materials and Methods:** The plant leaves were subjected to Soxhlet extraction followed by qualitative phytochemical screening and the separation of active constituents by applying column chromatography. The obtained fraction was subjected to spectral analysis to identify the compound. Molecular docking followed by *in vitro* enzyme assays were used to study the inhibitory effect of the isolated compound. **Results:** The plant leaves were used for the extraction, and the identified compound was *S-benzo[d]oxazol-2-yl 2-(piperazine-1-yl)ethanethioate*, confirmed by spectral analysis. From *in-silico* ADMET analysis, the isolated compound displayed most drug-likeness features, and in molecular docking studies, it has developed many crucial hydrogen bonding and hydrophobic interactions with enzymes (PDB IDs: 1V4S, 2P8S, 3BAX, and 3WY2). An *in vitro* enzyme assay validated the virtual screening results of isolated compounds. Isolated compound at 250 µgm/mL displayed 96.29±2.56, 89.23±2.1, 72.72±0.75, and 69.76±0.85% activity against GK, DPP-IV, alpha-amylase, and alpha-glucosidase enzymes, respectively. **Conclusion:** Our study concluded that DM could be treated using an isolated compound after further *in-vivo* and *in-vitro* studies.

Keywords: DPP-IV, *in-vitro*, *Rhus tripartite*, Isolation, Characterization.

Correspondence:
Dr. Anupama B
Department of Pharmaceutical Chemistry, K.V.S.R. Siddhartha College of Pharmaceutical Sciences, Andhra Pradesh, INDIA.
Email: khushiazeez@yahoo.co.in

Received: 21-09-2022;
Revised: 17-02-2023;
Accepted: 28-03-2023.

INTRODUCTION

Diabetes is associated with various clinical complications, including cardiovascular disease, retinopathy, nephropathy, and neuropathy.[1-3] The problem of Type 2 Diabetes Mellitus (T2DM), which affects people all over the globe, is becoming worse. Diabetes has increased dramatically in the US and the Middle East due to diet patterns, rapid development, and economic growth. In 2013, the prevalence of DM in Saudi Arabia was 382 million, projected to be 592 million by 2035.

The current oral care medications for T2DM are designed to lower the amount of glucose that is synthesized in the liver, increase the amount of glucose that is secreted, lower the amount of glucose that is consumed, and raise the amount of glucose that is used.[4-6] Biguanides, sulfonylureas, thiazolidinediones, meglitinides, and β-glucosidase inhibitors are the most frequent medications used to treat T2DM. However, most of these medications have common negative effects, such as weight gain and hypoglycemia.[7-9] Numerous new anti-diabetic medications have been developed to overcome these side effects, including 11b-hydroxysteroid dehydrogenase 1 inhibitors, sodium-glucose cotransporter 2 inhibitors, Dipeptidyl Peptidase IV (DPP-IV) inhibitors, and glucagon receptor antagonists.[10,11]

Inhibiting carbohydrate enzymes alpha-glucosidase and alpha-amylase reduces postprandial blood glucose rise significantly and may thus be an effective blood glucose management strategy for T2DM.[12] DPP-IV inhibition has proven to be a treatment for T2DM that is not only safe but also highly successful and well recognized.[4,13,14] The enzyme Glucokinase

DOI: 10.5530/ijper.57.2s.52

(GK) catalyzes the phosphorylation of glucose by serving as a glucose sensor in β-cells of the pancreas.[15,16] It acts as a regulating enzyme for glycogen formation and hepatic glucose clearance and is responsible for keeping the glucose level inside cells stable.[17,18] GKAs have recently been shown to be of great benefit to people who have type 2 diabetes, according to recent research.[19-23]

The hunt for novel pharmacologically active natural substances for treating human ailments may lead to the development of various clinically useful natural medicines. There exists a need to discover and develop some novel anti-diabetic agents, especially from natural sources, as they are significantly safer than synthetic drugs. The genus Rhus is primarily found in tropical, subtropical, and temperate zones. *Rhus tripartite* grows wild in Saudi Arabia's Hail region. The *Rhus tripartite* plant has been used in Arabian folk medicine to treat inflammatory conditions and GI and CV disorders for centuries. Polyphenols, flavonoids, proanthocyanidins, and other phytochemicals found in *Rhus* species are extensively employed in contemporary and traditional medicine. Antimicrobial, antitumorigenic, antioxidant, hypoglycemic, and anticonvulsant properties have been described for a *Rhus* extract. Given the crucial role of the above enzymes in treating DM, we aimed to study the inhibitory potential of a bioactive compound isolated from *Rhus tripartite* on these enzymes through molecular docking followed by *in vitro* enzyme assays.

MATERIALS AND METHODS

Collection of Plant Material and Authentication

The plants were identified, and fresh *Rhus tripartite* leaves were collected in Saudi Arabia's northeastern Hail region in March 2021. For authentication, the plant herbarium was submitted to the Department of Botany, Sri Venkateswara University, Tirupati, India.

Chemicals, Reagents, and Instruments

All the required chemicals and reagents, i.e., methanol, ethyl acetate, and sodium sulfate, were purchased and procured from Lab Trading Laboratory, Aurangabad, Maharashtra, India. The 100183-SND 400 MHz NMR instrument was used to generate ^{1}H and ^{13}C NMR graphs, whereas the LC-Ms Shimadzu Mass spectrometer was used to get Mass spectra. Tetramethylsilane (TMS) was used as an internal standard in NMR analysis.

Extraction and Isolation

The plant's leaves were left to dry naturally in the air at room temperature so that they wouldn't lose too much of their chemical components. The dried leaves were ground in a grinder to get a course powder for extraction. 1000 gm of course powder was extracted by Soxhlet apparatus using hydro-alcoholic solvents (methanol: water, 70:30) until the completion of at least 10-15 siphon cycles. A dry extract weighing 267 gm (26.7%) was obtained by passing it through a Whatmann No. 1 concentration filter while evaporating at 40°C in a rotary evaporator and operating under decreased pressure. We calculated the percentage yield using the weight of the plant materials after they had been air dried and the amount of the extract produced after drying.

The 100 gm of the above dry extract was mixed with 500 mL of distilled water and extracted with Ethyl Acetate (EtOAc) for 24 hr. The resulting extract was subjected to a second drying process using anhydrous sodium sulfate. The EtOAc fraction was concentrated at 35°C to get dry mass, which was then lyophilized to make it a free-flowing powder, which was given the code ETAF-1. A column made of borosilicate glass and measuring 30 centimeters in height was filled with silica gel before ETAF-1, weighing 10 gm was placed into the column. In gradient elution mode, the fraction was separated using mobile phases composed of various solvents. The mobile phases were 100% ethyl acetate, ethyl acetate: methanol (7:3), and 100% methanol. In the mobile phase, the 12 sub-fractions were produced using ethyl acetate: methanol (7:3). On these 12 fractions, TLC was performed using silica gel H plates to yield a chemical that appears in greater concentrations in the sub-fraction. In the TLC analysis of the above fractions, it was observed that fraction number-08 displayed only a single spot after visualization; therefore, only this fraction was subjected to further analysis. This isolated compound was subjected to ^{1}H NMR, ^{13}C NMR, and Mass spectrometry (LC-MS) analysis to elucidate the structure. After confirming the structure of the isolated molecule, an *in silico* ADMET analysis and molecular docking study were performed on various enzymes.

Virtual Screening of Isolated Compound

Pharmacokinetics and toxicity predictions of an isolated compound

ADMET properties play essential roles in discovering and developing new drugs. The drug candidate should demonstrate optimal ADMET characteristics at the therapeutic dosage. An isolated molecule was investigated for its ADME profile as well as its drug-likeness and toxicity criteria. Using the Swiss ADME server, the Lipinski Rule of five (LRo5) and the pharmacokinetic (ADME) characteristics of the isolated compound were studied.[24] ProTox-II is a site that can be accessed without cost and is used for making *in silico* toxicity predictions for novel derivatives. This web server was used to predict whether the molecule is poisonous or not (http://tox.charite.de/protox_II).

Molecular Docking

When carrying out the molecular docking process, the software programs Autodock Vina 1.1.2 and PyRx Virtual Screening Tool 0.8 from the Chimera version 1.10.2 and the Biovia Discovery Studio were used. The structure of the isolated compound, represented as an SDF file, was drafted using ChemDraw Ultra

version 12.0, and the structures of the naturally occurring ligands were obtained from the PubChem database maintained by the US National Library of Medicine. Energy reduction was carried out by using Universal Force Field (UFF).[25] The RCSB Protein Data Bank was consulted to get the enzymes' three-dimensional crystal structures (https://www.rcsb.org/). 3D ribbon view of selected enzymes with Native Ligand (NL) in the cavity is illustrated in Figure 1.

For molecular docking, the three-dimensional grid box of known size (Alpha-amylase, size_x = 55.5421 A^0, size_y = 58.2603A^0, size_z = 39.9963A^0; Alpha-glucosidase, size_x =25.0 A^0, size_y = 47.6775 A^0, size_z = 59.2180 A^0; DPP-IV, size_x = 67.1704 A^0, size_y = 72.2455 A^0, size_z = 63.6575 A^0; and GK, size_x = 67.1704 A^0, size_y = 72.2455 A^0, size_z = 63.6575 A^0; was adjusted (to define area for interactions) with exhaustiveness value of 8. There were active amino acid residues found by using the BIOVIA Discovery Studio Visualizer. The complete molecular docking technique, including identifying cavity and active amino acid residues, was carried out using the strategy described by Khan *et al.*[26-34]

In vitro Enzyme Assay

GK activation assay

Sigma-Aldrich was the vendor for the glucokinase enzyme extracted from *Bacillus stearothermophilus*. The isolated compound was put through an *in vitro* test to see whether or not it was successful in the activation of GK. This test, known as an SC_{50} test, evaluated the molecule's activity using a concentration of 50 µM across the board. An isolated compound was put through a series of tests with varying concentrations ranging from 50 to 250 µM on a 96-well plate with a final reaction volume of 100 µl. As the reaction mixture, we used the following components: 25 mM Hepes with a pH of 7.5, 10 mM glucose, 1 mM ATP, 4 U/mL G6PDH (Sigma-Aldrich), 1 mM NADP, 2.5 mM MgCl2, 50 mM KCl, 2 mM DTT, 1 mM glucokinase, and the isolated compound. The reaction mixtures were held at a temperature lower than

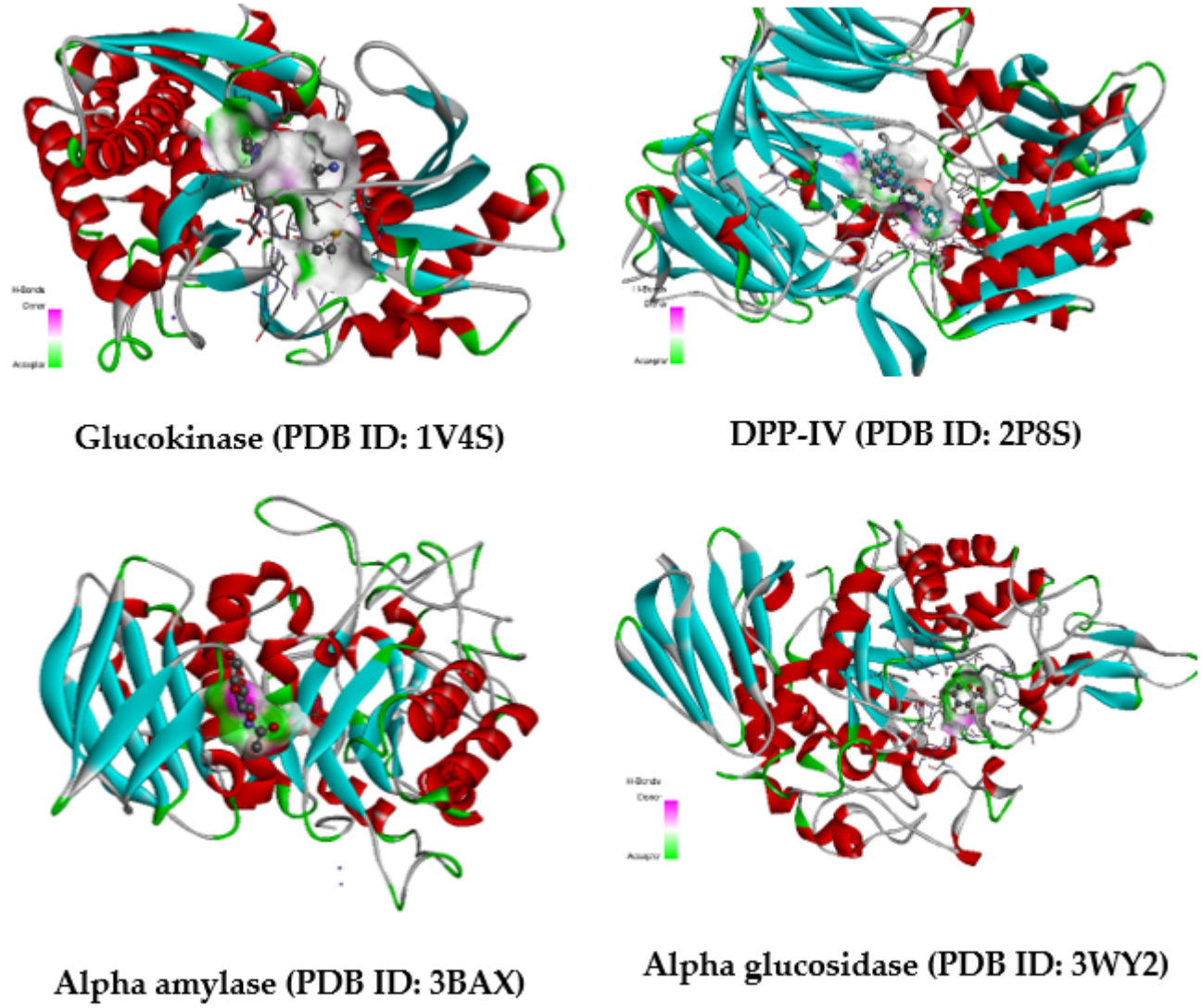

Figure 1: Three-dimensional view of selected enzymes with NL in the cavity along with PDB IDs.

37 degrees Celsius for twenty minutes. Kinetic analysis was performed at a wavelength of 340 nm to follow the rate of rising absorbance of NADPH that was liberated during the reaction. To ascertain the values, a comparison was made between them and GK, which had not been treated in any way. This aspect of the stimulatory concentration (SC_{50}) is known as its effectiveness.[35,36]

DPP-IV inhibition assay

The N-terminal dipeptidase serine protease is known as DPP-IV. In this particular piece of research, an isolated compound was put through an *in vitro* DPP-IV enzyme test. H-Gly-Pro-7-amino-4-methyl coumarin, also known as H-Gly-Pro AMC, served as a surrogate substrate to measure the level of DPP-IV activity. Vildagliptin served as the standard. DPP-IV cleaves the peptide bond, which causes the release of the AMC group. This results in fluorescence spectrophotometrically measured at a wavelength of 562 nm. The absorbance of the half-maximal inhibitory concentration was determined. The process was done three times in total.[37]

α-amylase and α-glucosidase inhibition assay

In the current investigation, the drug acarbose served as the control. In a test tube, 1 mL of alpha-amylase and 1 mL of the separated fraction were subjected to an incubation period of ten minutes at 37°C. After the tubes had been pre-incubated, 1 mL of a 1% (v/v) starch solution was added to each one, and the tubes were then heated to 37°C for 15 min. After adding 2 mL of DNSA reagent to halt the reaction, the mixture was heated in a boiling water bath for 5 min, cooled, and diluted, and the absorbance was measured using a spectrophotometer set at 546 nm (Shimadzu). During the control procedure, no fraction could be separated. Hence, the total enzyme activity was 100%. In order to conduct an alpha-glucosidase inhibition experiment, the same technique was repeated, but this time the absorbance was measured at 405 nm. The various isolated fractions and acarbose concentrations, ranging from 2 mg/mL to 16 mg/mL, were measured.[38] Alpha-glucosidase and alpha-amylase % inhibition by isolated fraction and acarbose may be calculated:

$$\% \text{ inhibition} = \frac{\text{Enzyme activity of control} - \text{Enzyme activity of extract}}{\text{Enzyme activity of control}} \times 100$$

RESULTS

The predicted and actual ^{1}H NMR spectrum and structure are illustrated in Figure 2. Predicted and experimentally obtained ^{13}C NMRs of the isolated compound are exemplified in Figure 3, along with structure and numbering. The compound's mass spectra are given in Figure 4, with fragment structure near the obtained respective peaks.

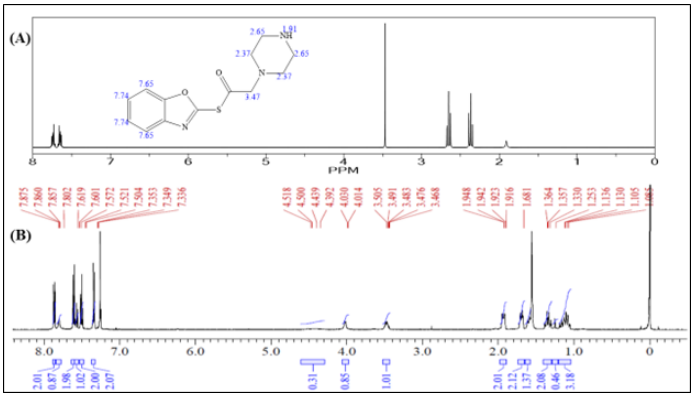

Figure 2: ^{1}H NMR spectrum of the isolated compound; A) Predicted ^{1}H NMR by ChemDraw Ultra 12.0; B) Experimental ^{1}H NMR of the isolated compound.

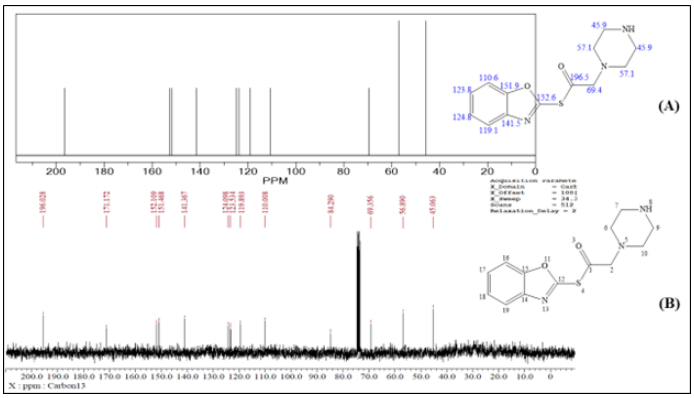

Figure 3: ^{13}C NMR spectrum of the isolated compound; A) Predicted ^{13}C NMR by ChemDraw Ultra 12.0; B) Experimental ^{13}C NMR of the isolated compound.

The LRo5 and Veber's properties of isolated compounds and NL present in the selected crystal structures of enzymes are tabulated in Table 1. The pharmacokinetics and drug-likeness of isolated compounds and NL are given in Table 2. The acute toxicity of an isolated compound was predicted and compared with NL. The predicted acute toxicity of the molecules is illustrated in Table 3.

The docking scores, active amino acid residues, bond length, and bond categories of isolated compound with all the selected enzymes are tabulated in Table 4. The 2D- and 3D-docking orientations of isolated compound with enzymes are exemplified in Table 5.

DISCUSSION

Structural elucidation of the isolated compound

The different spectrums obtained experimentally were compared with the spectrum of compounds suggested by HR-MS analysis. From spectral data, the interpreted structure was *S-benzo[d]oxazol-2-yl 2-(piperazine-1-yl)ethanethioate*; the spectral data with compound structure is described below:

Mol. formula: $C_{13}H_{15}N_3O_2S$; mol. Wt.: 277 gm/mol; R_f value: 0.82. Elemental analysis (*calc.*): C, 56.30; H, 5.45; N, 15.15; O, 11.54; S, 11.56.

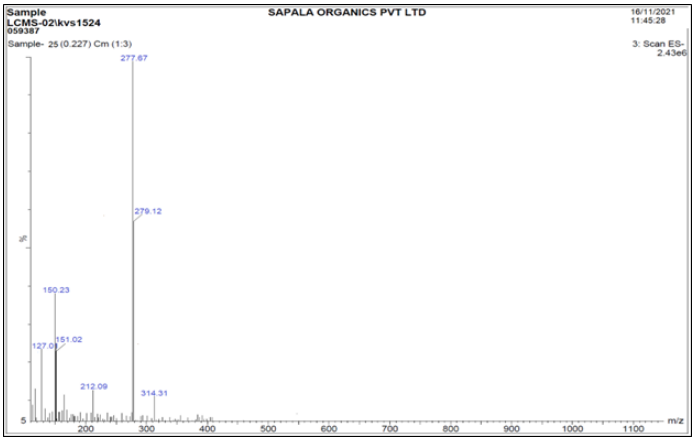

Figure 4: The mass spectra of the isolated compound.

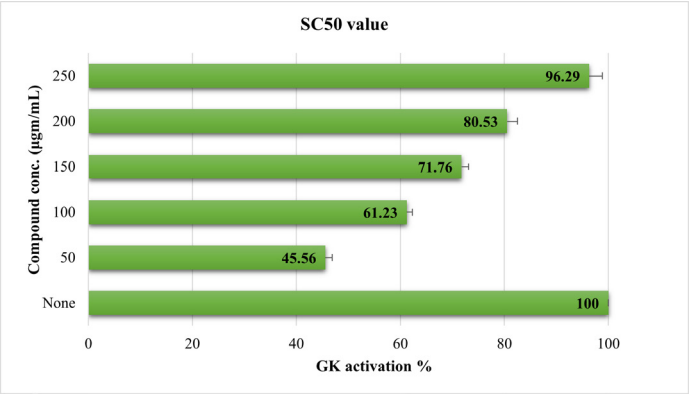

Figure 5: GK enzyme assay of the isolated compound

^{1}H NMR (400 MHz, DMSO-d_6, chemical shift (ppm)): δ 1.91 (*s*, NH of diazine), 1.923 (*s*, protons of C_6 and C_{10}), 1.942, 1.948 (*d*, protons of C_7 and C_9), 3.476 (*s*, protons of C_2), 7.601, 7.619 (*d*, protons of C_{16} and C_{19}), 7.802, 7.857 (*d*, protons of C_{17} and C_{18}).

^{13}C NMR (400 MHz, DMSO-d_6, chemical shift (ppm)): 45.063 (C_7 and C_9), 56.890 (C_6 and C_{10}), 69.356 (C_2), 110.008 (C_{16}), 119.893 (C_{19}), 123.534 (C_{17}), 124.098 (C_{18}), 141.367 (C_{14}), 151.468 (C_{15}), 152.109 (C_{12}), 196.028 (C_1).

MS: m/z 277.67, 279.12 (m+1), 127.01(fragment-1), 150.23 (fragment-2).

Pharmacokinetics and toxicity predictions of the isolated compound

The investigation of ADME features of a novel compound helps to study and explain how pharmacokinetic processes occur. None of the molecules have disobeyed the LRo5 or the Veber rule, as seen in Table , which indicates that these rules have been followed correctly. Lipophilicity is a vital property determining how a molecule functions inside the body. It is defined by Log-P of the compounds, which assesses the permeability of medicament in the biological system in order for it to reach the target tissue.[39] The log P values of the isolated compound were found to be 1.48, which indicates optimum lipophilicity. The fact that all of the molecules, including the isolated compound, had a molecular weight of less than 500 Da demonstrates that they are able to pass across biological membranes with relative ease and facilitates active transport.[26] It has been discovered that the Total Polar Surface Area (TPSA) and the number of rotatable bonds are better able to differentiate between compounds that are or are not active when taken orally. Veber's rule dictates that the TPSA should be less than 140, and the number of rotatable bonds should be less than 10. An isolated compound did not violate any of the above-discussed rules.

These compounds' drug-likeness and pharmacokinetics features were analyzed and modeled to optimize the molecules better. The isolated compound showed no evidence of penetrating the Blood-Brain Barrier (BBB), a desirable quality for a medicine that will treat conditions other than those affecting the CNS. The isolated compound's bioavailability and log *Kp* (skin penetration, cm/s) values were within an acceptable limit. Isolated compound displayed high GI absorption, whereas native ligands of 1v4s, 3bax, and 3wy2 exhibited GI absorption. GI absorption is very crucial for the development of oral dosage forms. An isolated compound displayed CYP1A2 and CYP2C19 inhibitory potential, which indicates that it might interfere with the metabolism of other drugs, but fortunately, it did not show inhibition of CYP2C9, CYP2D6, and CYP3A4. The isolated compound did not violate any of the Ghose, Egan, and Muegge rules, which indicates it has the most drug-likeness properties (Table).

In acute toxicity predictions, isolated compound and native ligands of 1v4s and 2ps8 fall in toxicity class IV, indicating that it is harmful if ingested($300<LD_{50}\leq2000$). The native ligand of 3bax fall in toxicity class V, which indicates that there is a potential for damage if the substance is ingested ($2000<LD_{50}\leq5000$).[40] The native ligand of 3wy2 fall in toxicity class-VI, which indicates non-toxic compounds. An isolated compound did not show carcinogenicity, hepatotoxicity, immunotoxicity, cytotoxicity, and mutagenic properties. The results of this virtual screening encouraged us to the conclusion that an isolated chemical has drug-like qualities. As a result, the compound was put through molecular docking experiments to achieve a higher optimization level.

Molecular docking

Molecular docking is a computational method that allows us to digitally screen molecules to determine the ligand's preliminary activity potential against biological targets. Here, we have investigated the inhibitory potential of molecular docking on α-amylase, α-glucosidase, DPP-IV, and GK, as these are essential targets for developing novel anti-diabetic drugs. The binding affinities of an isolated compound with all the enzymes with crystal structures 1v4s, 2ps8, 3bax, and 3wy2 are discussed in the below section. The isolated molecule had a binding free energy of -5.8 kcal/mol when docked with 1v4s. Additionally, it formed one

Table 1: **Veber's rule and the LRo5 were computed for NLs and isolated compound.**

Compound codes	LRo5					Veber's rule	
	Log P	Mol. Wt.	H	BA. HBD.	Violations	TPSA (Å^2)	No. of rotatable bonds
Isolated compound.	1.48	277.34	5	1	0	83.67	4
NL (1v4s)	2.29	349.41	4	2	0	139.37	5
NL (2ps8)	3.29	419.37	10	1	0	59.97	3
NL (3bax)	-1.78	221.21	6	5	0	119.25	3
NL (3wy2)	-2.16	180.16	6	5	0	110.38	1

Table 2: **NL and isolated molecules' pharmacokinetic and drug-like features.**

Parameters		Isolated compound.	NL (1v4s)	NL (2ps8)	NL (3bax)	NL (3wy2)
Pharmacokinetics	GI absorption	High	Low	High	Low	Low
	BBB permeation	-	-	Yes	-	-
	P-gp substrate	-	-	Yes	Yes	Yes
	CYP1A2 inhibition	Yes	Yes	-	-	-
	CYP2C19 inhibition	Yes	Yes	-	-	-
	CYP2C9 inhibition	-	Yes	-	-	-
	CYP2D6 inhibition	-	Yes	Yes	-	-
	CYP3A4 inhibition	-	Yes	-	-	-
	Log K_p (skin permeation, cm/s)	-6.71	-6.59	-7.43	-8.47	-9.7
Drug-likeness	Ghose	0	0	0	1	2
	Egan	0	1	0	0	0
	Muegge	0	0	0	0	2
	Bioavailability Score	0.55	0.55	0.55	0.55	0.55

Table 3: **The estimated values of acute toxicity for native ligands and the isolated compound.**

Parameters	Compound names				
	Isolated compound.	NL (1v4s)	NL (2ps8)	NL (3bax)	NL (3wy2)
LD_{50} (mg/kg)	1000	1000	1000	5000	23000
Toxicity class	4	4	4	5	6
Prediction accuracy (%)	54.26	54.26	23	69.26	67.38
Hepatotoxic (Probability)	IA (0.65)	A (0.65)	IA (0.59)	IA (0.72)	IA (0.98)
Carcinogenic (Probability)	IA (0.59)	A (0.56)	IA (0.51)	IA (0.71)	IA (0.82)
Immunotoxic (Probability)	IA (0.97)	IA (0.83)	IA (0.65)	IA (0.99)	IA (0.99)
Mutagenic (Probability)	IA (0.59)	IA (0.53)	IA (0.54)	IA (0.72)	IA (0.81)
Cytotoxic (Probability)	IA (0.75)	IA (0.71)	IA (0.66)	IA (0.69)	IA (0.87)

Where, IA: Inactive; A: Active.

Table 4: The molecular interactions of isolated compound with target enzymes.

Active amino acid residues	Bond length (Å)	Bond type	Bond category	Docking scores (Kcal/mol)
1v4s				
LYS296	1.83659	Hydrogen Bond	Conventional Hydrogen Bond	-5.8
GLY328	3.71871		Carbon Hydrogen Bond	
GLU300	4.05797	Electrostatic	Pi-Anion	
GLU300	4.3812			
VAL277	5.20169	Hydrophobic	Pi-Alkyl	
ARG327	5.2948			
2p8s				
HIS100	2.25273	Hydrogen Bond	Conventional Hydrogen Bond	-7.1
ASN92	2.32368			
ILE102	3.98355	Hydrophobic	Pi-Sigma	
PHE95	5.19679		Pi-Pi T-shaped	
ILE102	5.01272		Pi-Alkyl	
3bax				
HIS201	2.55706	Hydrogen Bond	Conventional Hydrogen Bond	-6.6
GLU233	3.55406		Carbon Hydrogen Bond	
GLU233	3.48394			
GLU233	3.36948			
TRP59	5.58568	Hydrophobic	Pi-Pi Stacked	
TRP59	5.33456			
TYR62	5.83625		Pi-Pi T-shaped	
LEU165	5.14923			
LEU165	5.44646			
3wy2				
GLU283	2.32571	Hydrogen Bond	Conventional Hydrogen Bond	-5.5
HIS240	2.35562			
ARG246	2.41067			
VAL241	3.74246	Hydrophobic	Pi-Sigma	
VAL241	3.84853		Pi-Alkyl	
ARG239	4.88229			

conventional hydrogen bond and one carbon-hydrogen bond with Lys296 and Gly328. Electrostatic interactions of the Pi-anion type were observed between Glu300 and this compound. In addition, it exhibited the pi-alkyl form of hydrophobic interactions with Arg327 and Val277. It formed two conventional hydrogen bonds with His100 and Asn92 and had a binding free energy of-7.1 kcal/mol when interacting with 2p8s. In addition, it has established hydrophobic interactions with Ile102 and Phe95 in the form of pi-sigma and pi-pi T-shaped interactions. It had binding free energy of -6.6 kcal/mol when docked with 3bax, and it generated one conventional hydrogen bond and three carbon-hydrogen bonds with His201 and Glu233. Electrostatic interactions of the Pi-anion type were observed between Glu300 and this compound. In addition, it demonstrated hydrophobic interactions of the pi-pi stacked and pi-pi T-shaped types with Trp59, Trp62, and Leu165. It established three conventional hydrogen bonds with Glu283, His240, and Arg246 and displayed a binding affinity of -5.5 kcal/mol with 3wy2. Pi-sigma and Pi-alkyl interactions were created between it and Arg239 and Val241. From docking investigations it was observed that –NH group is playing crucial role in the formation of close bonds with the targets.

GK enzyme assay

In vitro GK enzyme assay revealed that isolated compound exhibit optimum GK activation potential in a dose-dependent manner

Table 5: The 2D- and 3D molecular postures of the isolated compound.

2D-binding orientations	3D-binding orientations
1v4s	
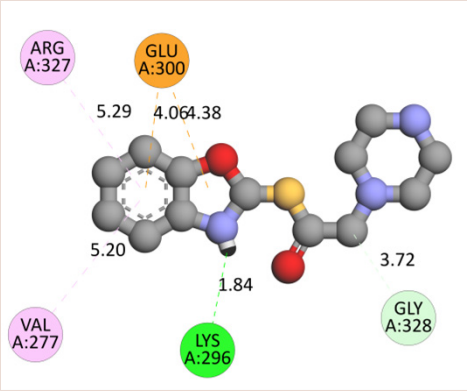	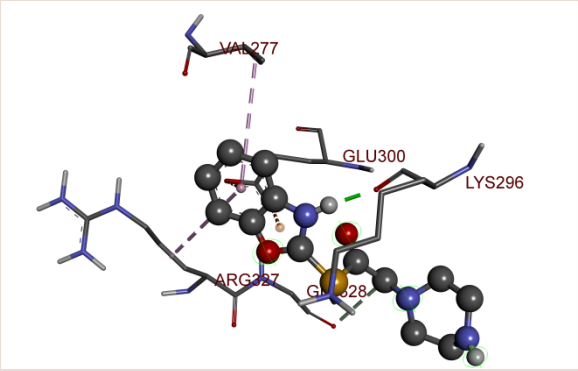
2ps8	
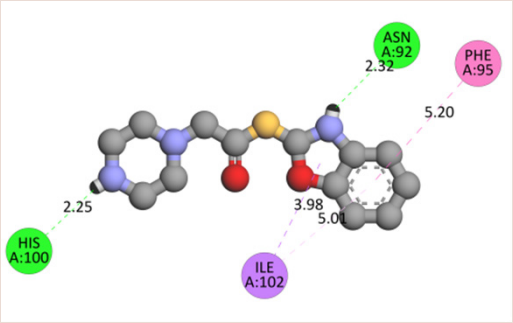	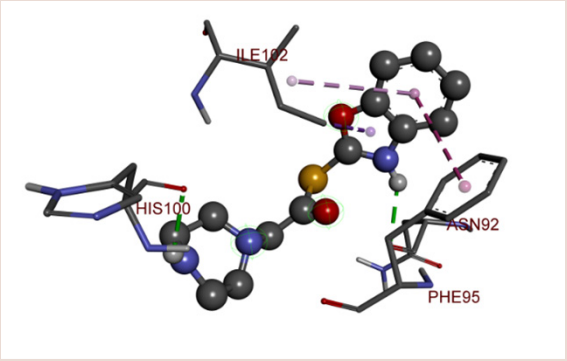
3bax	
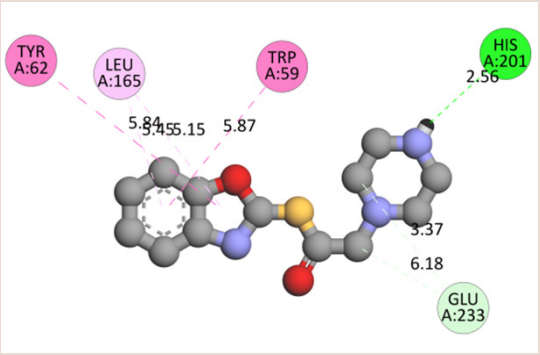	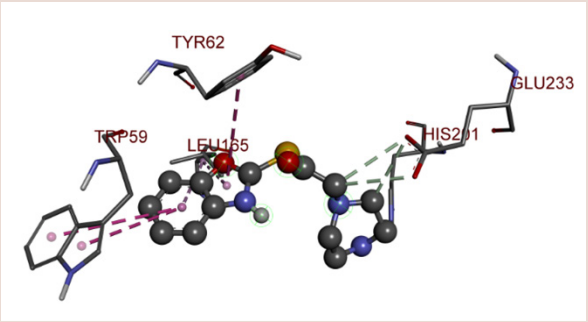
3wy2	
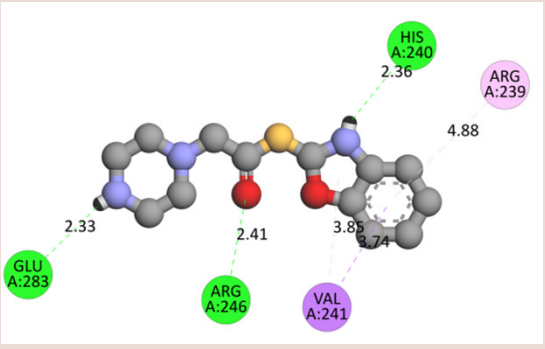	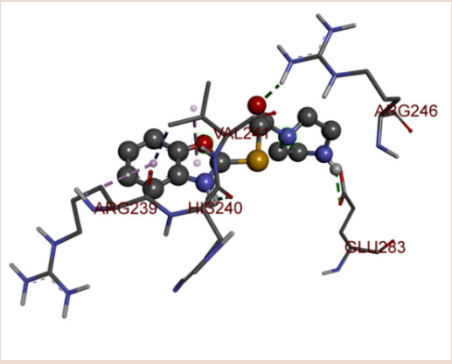

Table 6: The % of enzymes alpha-amylase and alpha-glucosidase that were inhibited by the compound.

Concentrations (µgm/mL)	Isolated compound		Acarbose	
	% inhibition		% inhibition	
	alpha-amylase	alpha glucosidase	alpha amylase	alpha-glucosidase
50	NA*	NA*	32.93±0.80	30.63±0.83
100	23.36±0.33	20.96±0.43	48.83±0.34	47.33±0.54
150	41.53±0.41	38.83±0.71	72.74±0.82	67.78±0.89
200	58.87±0.24	52.37±0.94	89.71±0.95	85.61±0.92
250	72.72±0.75	69.76±0.85	97.42±0.92	98.92±0.82

(Figure 5). It displayed maximum GK activation at 250 µgm/mL, i.e., 96.29±2.56%.

DPP-IV enzyme assay

DPP-IV enzyme assay revealed that the isolated compound demonstrated comparative activity with standard drug sitagliptin at different concentrations (50-250 µgm/mL, Figure 6). Isolated compound displayed 89.23±2.1% inhibition at 250 µgm/mL concentration, whereas sitagliptin showed 99.92±1.12% at the same concentration.

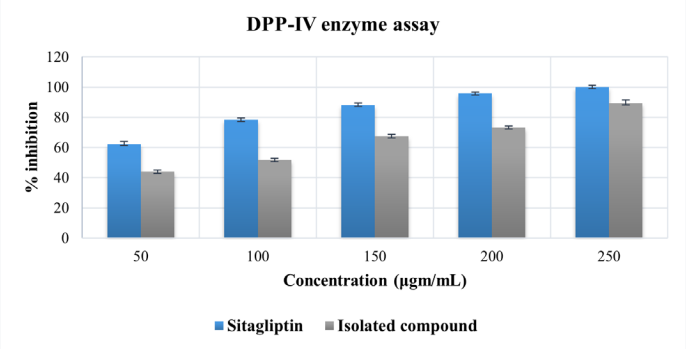

Figure 6: DPP-IV enzyme assay of the isolated compound.

alpha-amylase and alpha-glucosidase enzyme assay

Table 6 is a tabulation of the percent inhibition of the alpha-amylase and alpha-glucosidase enzymes. Acarbose was used as a control so that the inhibitory effects of the isolated compound could be compared to those of a known compound. The results showed that the isolated compound stopped the alpha-amylase and alpha-glucosidase enzymes from working very well. The isolated compound at 250 µgm/mL displayed 72.72±0.75 and 69.76±0.85, inhibiting alpha-amylase and alpha-glucosidase enzymes, respectively. The most interestingly isolated compound was not active at 50 µgm/mL of concentration against both enzymes.

CONCLUSION

Scientists have found that chemicals made from plants can be used in different ways in medicine, pharmacy, and general biology. These compounds come from a wide variety of plant sources. Researchers have predicted that screening natural resources would create new 'lead' compounds due to the immense structural variety of natural goods and the relevance of natural products to the pharmaceutical industry. It is well known that structural analogs with higher pharmacological activity and fewer adverse effects may be formed by modifying the functional groups of such lead compounds at the molecular level. Compounds obtained from a wide variety of natural product sources have served as the foundation for creating therapeutically relevant drugs that are active against various disorders. Given the crucial role of GK, DPP-IV, alpha-amylase, and alpha-glucosidase enzymes in treating DM, we aimed to study the inhibitory potential of a bioactive compound isolated from *Rhus tripartite* on these enzymes through molecular docking followed by *in vitro* enzyme assays. The identified compound was *S-benzo[d]oxazol-2-yl 2-(piperazine-1-yl)ethanethioate*, which was confirmed by spectral analysis. The present compound demonstrated excellent activity and displayed the most drug-like properties. From the present investigation, we concluded that isolated compounds could be used clinically to treat DM, but before that, numerous clinical data points need to be generated from many *in vivo* and *in vitro* models. Also, one can consider this nucleus as a lead molecule for the further development of novel anti-diabetic compounds.

ACKNOWLEDGEMENT

Scientific Research Deanship at the University of Ha'il – Saudi Arabia, through project number RD-21 133, has funded this research.

CONFLICT OF INTEREST

The authors declare that there is no conflict of interest.

ABBREVIATIONS

GK: Glucokinase; **DPP-IV:** Dipeptidyl peptidase; **T2DM:** Type 2 diabetes mellitus; **TMS:** Tetramethylsilane; **ADMET:** Absorption, distribution, metabolism, excretion, and toxicity; **NL:** Native ligand; **α:**Alpha; **TPSA:**Total polar surface area; **IA:** Inactive; **A:** Active; **GI:** absorption; **P-gp sub:** p-glycoprotein substrate; **BBB:** Blood-brain barrier.

SUMMARY

The Glucokinase (GK), Dipeptidyl Peptidase-IV (DPP-IV), alpha-glucosidase, and alpha-amylase enzymes play an important role in the treatment of Type 2 Diabetes Mellitus (T2DM). Given the crucial role of the above enzymes in treating DM, we aimed to study the inhibitory potential of a bioactive compound isolated from *Rhus tripartite* on these enzymes through molecular docking followed by *in vitro* enzyme assays. The plant leaves were used for the extraction, and the identified compound was *S-benzo[d]oxazol-2-yl 2-(piperazine-1-yl)ethanethioate*, confirmed by spectral analysis. From *in-silico* ADMET analysis, the isolated compound displayed most drug-likeness features, and in molecular docking studies, it has developed many crucial hydrogen bonding and hydrophobic interactions with enzymes (PDB IDs: 1V4S, 2P8S, 3BAX, and 3WY2). An *in vitro* enzyme assay validated the virtual screening results of isolated compounds. Isolated compound at 250 µgm/mL displayed 96.29±2.56, 89.23±2.1, 72.72±0.75, and 69.76±0.85% activity against GK, DPP-IV, alpha-amylase, and alpha-glucosidase enzymes, respectively.

REFERENCES

1. Li N, Wang LJ, Jiang B, Guo SJ, Li XQ, Chen XC, *et al*. Design, synthesis and biological evaluation of novel pyrimidinedione derivatives as DPP-4 inhibitors. Bioorg Med Chem Lett. 2018;28(12):2131-5. doi: 10.1016/j.bmcl.2018.05.022, PMID 29773502.
2. Alanazi M, Unnisa A, Patel RD, Alanazi J, Khalid M, Ahmad S, Jandrajupalli SB, *et al*. Comparative analysis between mono approach and multi approaches in managing T2DM: a survey-based study. Eur Rev Med Pharmacol Sci. 2022;26(17):6290-9. doi: 10.26355/eurrev_202209_29653, PMID 36111930.
3. Sharma M, Gupta M, Singh D, Kumar M, Kaur P. Synthesis, evaluation and molecular docking of Thiazolopyrimidine derivatives as dipeptidyl peptidase IV inhibitors. Chem Biol Drug Des. 2012;80(6):918-28. doi: 10.1111/cbdd.12041, PMID 22943413.
4. Gallwitz B. Clinical use of DPP-4 inhibitors. Front Endocrinol. 2019;10:389. doi: 10.3389/fendo.2019.00389, PMID 31275246.
5. Tsai TY, Hsu T, Chen CT, Cheng JH, Chiou MC, Huang CH, *et al*. Rational design and synthesis of potent and long-lasting glutamic acid-based dipeptidyl peptidase IV inhibitors. Bioorg Med Chem Lett. 2009;19(7):1908-12. doi: 10.1016/j.bmcl.2009.02.061, PMID 19269819.
6. Olokoba AB, Obateru OA, Olokoba LB. Type 2 diabetes mellitus: a review of current trends. Oman Med J. 2012;27(4):269-73. doi: 10.5001/omj.2012.68, PMID 23071876.
7. Narsimha S, Battula KS, Ravinder M, Reddy YN, Nagavelli VR. Design, synthesis and biological evaluation of novel 1,2,3-triazole-based xanthine derivatives as DPP-4 inhibitors. J Chem Sci. 2020;132(1). doi: 10.1007/s12039-020-1760-0.
8. Abd El-Karim SS, Anwar MM, Syam YM, Nael MA, Ali HF, Motaleb MA. Rational design and synthesis of new tetralin-sulfonamide derivatives as potent anti-diabetics and DPP-4 inhibitors: 2D and 3D QSAR, *in vivo* radiolabeling and biodistribution studies. Bioorg Chem. 2018;81:481-93. doi: 10.1016/j.bioorg.2018.09.021, PMID 30243239.
9. Han B, Liu JL, Huan Y, Li P, Wu Q, Lin ZY, *et al*. Design, synthesis and primary activity of thiomorpholine derivatives as DPP-IV inhibitors. Chin Chem Lett. 2012;23(3):297-300. doi: 10.1016/j.cclet.2011.12.007.
10. Pereira ALE, dos Santos GB, Franco MSF, Federico LB, da Silva CHTP, Santos CBR. Molecular modeling and statistical analysis in the design of derivatives of human dipeptidyl peptidase IV. J Biomol Struct Dyn. 2018;36(2):318-34. doi: 10.1080/07391102.2016.1277163, PMID 28027711.
11. Patel BD, Bhadada SV, Ghate MD. Design, synthesis and anti-diabetic activity of triazolotriazine derivatives as Dipeptidyl Peptidase-4 (DPP-4) inhibitors. Bioorg Chem. 2017;72:345-58. doi: 10.1016/j.bioorg.2017.03.004, PMID 28302310.
12. Tundis R, Loizzo MR, Menichini F. Natural products as α-Amylase and α-Glucosidase inhibitors and their hypoglycaemic potential in the treatment of diabetes: an update. Mini Rev Med Chem. 2010;10(4):315-31. doi: 10.2174/138955710791331007.
13. Scheen AJ. Safety of dipeptidyl peptidase-4 inhibitors for treating type 2 diabetes. Expert Opin Drug Saf. 2015;14(4):505-24. doi: 10.1517/14740338.2015.1006625, PMID 25630605.
14. Tella SH, Rendell MS. DPP-4 inhibitors: focus on safety. Expert Opin Drug Saf. 2015;14(1):127-40. doi: 10.1517/14740338.2015.977863, PMID 25488788.
15. Kamata K, Mitsuya M, Nishimura T, Eiki JI, Nagata Y. Structural basis for allosteric regulation of the monomeric allosteric enzyme human glucokinase. Structure. 2004;12(3):429-38. doi: 10.1016/j.str.2004.02.005, PMID 15016359.
16. Agius L. Glucokinase and molecular aspects of liver glycogen metabolism. Biochem J. 2008;414(1):1-18. doi: 10.1042/BJ20080595, PMID 18651836.
17. Iynedjian PB. Molecular physiology of mammalian glucokinase. Cell Mol Life Sci. 2009;66(1):27-42. doi: 10.1007/s00018-008-8322-9, PMID 18726182.
18. Irwin DM, Tan H. Evolution of glucose utilization: glucokinase and glucokinase regulator protein. Mol Phylogenet Evol. 2014;70(1):195-203. doi: 10.1016/j.ympev.2013.09.016, PMID 24075984.
19. Coghlan M, Leighton B. Glucokinase activators in diabetes management. Expert Opin Investig Drugs. 2008;17(2):145-67. doi: 10.1517/13543784.17.2.145, PMID 18230050.
20. Pal M. Recent advances in glucokinase activators for the treatment of type 2 diabetes. Drug Discov Today. 2009;14(15-16):784-92. doi: 10.1016/j.drudis.2009.05.013, PMID 19520181.
21. Matschinsky FM, Zelent B, Doliba N, Li C, Vanderkooi JM, Naji A, *et al*. Glucokinase activators for diabetes therapy: May 2010 status report. Diabetes Care. 2011;34;Suppl 2:S236-43. doi: 10.2337/dc11-s236, PMID 21525462.
22. Matschinsky FM, Porte D. Glucokinase Activators (GKAs) promise a new pharmacotherapy for diabetics. F1000 Med Rep. 2010;2(1). doi: 10.3410/M2-43, PMID 20948841.
23. Filipski KJ, Futatsugi K, Pfefferkorn JA, Stevens BD. Glucokinase activators. Pharm Pat Anal. 2012;1(3):301-11. doi: 10.4155/ppa.12.26, PMID 24236843.
24. Daina A, Michielin O, Zoete V. SwissADME: a free web tool to evaluate pharmacokinetics, drug-likeness and medicinal chemistry friendliness of small molecules [sci rep] [internet]. Sci Rep. 2017 May 3;7(1):42717. doi: 10.1038/srep42717, PMID 28256516.
25. Rappé AK, Casewit CJ, Colwell KS, Goddard WA, Skiff WM. UFF, a full periodic table force field for molecular mechanics and Molecular Dynamics simulations. J Am Chem Soc. 1992;114(25):10024-35. doi: 10.1021/ja00051a040.
26. Shntaif AH, Khan S, Tapadiya G, Chettupalli A, Saboo S, Shaikh MS, *et al*. Rational drug design, synthesis, and biological evaluation of novel N-(2-arylaminophenyl)-2,3-diphenylquinoxaline-6-sulfonamides as potential antimalarial, antifungal, and antibacterial agents. Digi. Chin Med. 2021;4(4):290-304. doi: 10.1016/j.dcmed.2021.12.004.
27. Siddiqui FA, Khan SL, Marathe RP, Nema NV. Design, synthesis, and *in silico* studies of novel N-(2-aminophenyl)-2,3-Diphenylquinoxaline-6-Sulfonamide derivatives targeting Receptor-Binding Domain (RBD) of SARS-CoV-2 spike glycoprotein and their evaluation as antimicrobial and antimalarial agents. Lett Drug Des Discov. 2021;18(9):915-31. doi: 10.2174/1570180818666210427095203.
28. Unnisa A, Khan SL, Sheikh FAH, Mahefooz S, Kazi AA, Siddiqui FA, *et al. In-silico* inhibitory potential of Triphala constituents against cytochrome P450 2E1 for the prevention of thioacetamide-induced hepatotoxicity.
29. Khan SL, Siddiqui FA, Shaikh MS, Nema NV, Shaikh AA. Discovery of potential inhibitors of the Receptor-Binding Domain (RBD) of pandemic disease-causing SARS-CoV-2 Spike glycoprotein from Triphala through molecular docking. Curr Chin Chem. 2021;01.
30. Khan S, Kale M, Siddiqui F, Nema N. Novel pyrimidine-benzimidazole hybrids with antibacterial and antifungal properties and potential inhibition of SARS-CoV-2 main protease and spike glycoprotein. Digi. Chin Med. 2021;4(2):102-19. doi: 10.1016/j.dcmed.2021.06.004.
31. Khan A, Unnisa A, Sohel M, Date M, Panpaliya N, Saboo SG, *et al*. Investigation of phytoconstituents of *Enicostemma littorale* as potential glucokinase activators through molecular docking for the treatment of type 2 diabetes mellitus. *In silico* Pharmacol. 2022;10(1):1. doi: 10.1007/s40203-021-00116-8, PMID 34926125.
32. Khan SL, Sonwane GM, Siddiqui FA, Jain SP, Kale MA, Borkar VS. Discovery of naturally occurring flavonoids as human cytochrome P450 (CYP3A4) inhibitors with the aid of computational chemistry. Indo Glob J Pharm Sci. 2020;10(4):58-69. doi: 10.35652/IGJPS.2020.10409.
33. Chaudhari RN, L.khan SL, Chaudhary RS, Jain SP, Sidduqui FA. B-sitosterol: isolation from *Muntingia calabura* Linn Bark extract, structural elucidation and molecular docking studies as potential inhibitor of SARS-CoV-2 Mpro (COVID-19). Asian J Pharm Clin Res. 2020;13(5):204-9. doi: 10.22159/ajpcr.2020.v13i5.37909.
34. Khan SL, Siddiui FA. Beta-sitosterol: as immunostimulant, antioxidant and inhibitor of SARS-CoV-2 spike glycoprotein. Arch Pharmacol Ther. 2020;2(1).
35. Min Q, Cai X, Sun W, Gao F, Li Z, Zhang Q, *et al*. Identification of mangiferin as a potential glucokinase activator by structure-based virtual ligand screening [sci rep]. Sci Rep. 2017;7:44681. doi: 10.1038/srep44681, PMID 28317897.
36. Kazi AA, Chatpalliwar VA. Design, synthesis, molecular docking and *in vitro* biological evaluation of benzamide derivatives as novel glucokinase activators. Curr Enzym Inhib. 2022;18(1):61-75. doi: 10.2174/1573408018666220218093451.
37. Niu P, Kang J, Tian X, Song L, Liu H, Wu J, *et al*. Synthesis of 2-amino-1,3,4-oxadiazoles and 2-amino-1,3,4-thiadiazoles via sequential condensation and I2-mediated

oxidative C-O/C-S bond formation. J Org Chem. 2015;80(2):1018-24. doi: 10.1021/jo502518c, PMID 25506709.

38. Poovitha S, Parani M. *In vitro* and *in vivo* α-amylase and α-glucosidase inhibiting activities of the protein extracts from two varieties of bitter gourd (*Momordica charantia* L.). BMC Complement Altern Med. 2016;16(Suppl 1):185. doi: 10.1186/s12906-016-1085-1, PMID 27454418.
39. Lipinski CA, Lombardo F, Dominy BW, Feeney PJ. Experimental and computational approaches to estimate solubility and permeability in drug discovery and development settings. Adv Drug Deliv Rev. 2012;46:4–17.
40. Banerjee P, Eckert AO, Schrey AK, Preissner R, ProTox II. ProTox-II: A webserver for the prediction of toxicity of chemicals. Nucleic Acids Res. 2018;46(W1):W257-63. doi: 10.1093/nar/gky318, PMID 29718510.

Cite this article: Unnisa A, Kunduru RD, Jandrajupalli SB, Elamine BA, Banu H, Anupama B, *et al*. Molecular Docking and *in vitro* Enzyme Assay of Bioactive Compound Isolated from *Rhus tripartite* as Potential Anti-Diabetic Agent. Indian J of Pharmaceutical Education and Research. 2023;57(2s):s442-s452.